J Mater Sci: Mater Electron (2015) 26:4234–4240
DOI 10.1007/s10854-015-2973-8

Microstructure and properties of Al/Sip composites for thermal management applications

Zhiyong Cai[1] · Richu Wang[1] · Chun Zhang[1] · Chaoqun Peng[1] · Linqian Wang[1]

Received: 23 October 2014 / Accepted: 17 March 2015 / Published online: 22 March 2015

Abstract Aluminum matrix composite reinforced with high amount of Si particle is an advanced electronic packaging material used in thermal management. In this work, Al/Sip composites with different Si contents were prepared by rapid solidification and hot pressing. Fine and homogeneous microstructures with defect-free were achieved, and no detrimental reaction was detected. The typical thermo-physical properties such as the thermal conductivity and coefficient of thermal expansion (CTE) of the Al/Sip composites were acceptable as electronic packaging material for semiconductor devices. The CTE increased gradually with the temperature. Additionally, the mechanical properties of the composites were measured. The technological performance (workability, platability, and laser weldability) of the composites were also evaluated.

1 Introduction

The continuous progress of microelectronic devices with high calculating speed within a more compact size leads to the rapid increase of power density [1, 2]. Previous data indicated that failure rate increases dramatically as device temperature increases, such as every 10 °C temperature rises, the lifetime of a GaAs or Si semiconductor device is reduced by a factor of three [3]. Therefore, development of materials with high thermal conductivity and tailored coefficient of thermal expansion (CTE) is imperative for heat sinks and heat spreaders [4]. Compatible CTE matching with those of semiconductor materials or ceramic substrates can minimize the thermally induced stresses and enhance the reliability of electronic components. Furthermore, superior thermal conductivity can favor heat dissipation to avoid the performance degradation or device failures.

Traditional metallic packaging materials, such as copper and aluminum, have good thermal conduction capability. However, their CTE are much higher than the desired ones for the attachment of ceramic substrates and semiconductors, limiting the long-term reliability of electronic devices. Compatible CTE and favorable thermal conductivity are achieved by Cu/W and Cu/Mo composites, but these composites have weight penalty and poor solderability [5]. Nowadays, great attentions have been paid to the lightweight aluminum matrix composites (AMCs), such as Al/SiC [6] and Al/AlN [7], attributes to the low density, isotropic microstructure, tailorable thermo-physical properties, and good mechanical properties. However, the poor wettability between the ceramic phase and matrix along with unwanted reaction products at the interface could lead to difficulty in fabrication, and hence deterioration of the thermo-mechanical properties [8].

Recently, Al/Sip composites with high Si content have become considerable interest as candidate advanced electronic packaging material because of their excellent properties such as low CTE, high thermal conductivity, light weight, and improved mechanical properties (e.g., high specific stiffness and specific modulus) [9, 10]. The Si particles with an average size of 12.5 ± 0.1 μm was achieved in Al/50 wt% Sip composite produced by spray deposition [9]. In order to refine the Si particles, Al/Sip composites were fabricated by spark plasma sintering (SPS) at a temperature of 510 °C, and relative densities

✉ Richu Wang
rcwcsu@163.com

[1] School of Materials Science and Engineering, Central South University, Changsha 410083, People's Republic of China

higher than 99 % were obtained [1]. Improved tensile properties of Al/Sip composites were achieved by alloying with copper [10]. The rapid solidification (RS) technique is a cost-effective method to produce material with fine and uniform microstructure [11, 12]. In the present study, Al/Sip composites with different Si contents are fabricated by hot pressing method using gas-atomized pre-alloyed powder. The microstructure, thermo-physical, and mechanical properties of the composites are investigated. The Al/Sip composites are aimed at application on thermal management; therefore, special emphasis are also placed on the workability, platability, and laser weldability.

2 Experimental procedure

2.1 Composite preparation

Polycrystalline pure Si (99.9 wt%) with weight fraction of 27, 50, and 70 was inductively melted with pure Al (99.9 wt%) at 950, 1250, and 1400 °C, respectively. The molted alloy was poured into a pre-heated graphite tundish with an inner diameter of 3.5 mm, and perform at a pressure of 0.9 MPa. During atomization, a fine dispersion of droplets was formed when molten Al–Si alloy was impacted by a high energy nitrogen gas. Al–50Si pre-alloyed powder obtained possess complicated shapes, e.g., irregular teardrops, ellipsoid, or quasi-spherical (Fig. 1a). Figure 1b shows the cross-sectional microstructure of the pre-alloyed powder with particle size of about 30 μm. It can be seen that irregular primary Si particle with block-like and needle-like eutectic Si phase with various aspect ratios distribute homogeneously in the Al matrix.

The as-atomized powder was cold pressed under 300 MPa for 10 min into a compacts with relative densities from 72 to 78 % depending on the Si content. Then the green billets were fabricated by vacuum hot pressing performed in a graphite die with its inner walls coated with BN slurry. The maximum pressure was 45 MPa. The selected sintering temperature and holding time were 565 °C and 60 min, respectively. The heating rate was 15 °C min^{-1}. After sintering, the hot pressed specimens were furnace cooled to the room temperature. Hot pressed specimens were in the form of discs with diameter and thickness of 50 and 10 mm, respectively.

2.2 Composite characterization

Specimens used for microstructural observations were prepared by standard metallurgical methods, i.e., grinding on SiC abrasive papers and polishing with 1 μm diamond paste, followed by etching with Keller's reagent (1 vol% HF–1.5 vol% HCl–2.5 vol% HNO_3–95 vol% H_2O). The microstructure of the composite and morphology of the Si reinforcement phase were observed using a field-emission scanning electron microscope (FE-SEM, FEI QUANTA-200). Image analysis was carried out to measure the average size of the Si reinforcement. X-ray diffraction (XRD) analysis was carried out with a Rigaku D/Max2500VB+ diffractometer using Cu Kα radiation at a scan step of 0.08 (°) s^{-1} from 20° to 100°.

Both tensile and three point bending tests were performed at room temperature with an initial strain rate of 0.5 mm min^{-1} using an Instron testing machine. Tensile specimen with dog bone-shape circular (a gauge diameter of 5 mm and gauge length of 10 mm) and bending specimen with square shape (thickness, width, and length of 3, 10, and 50 mm, respectively) were used. The Brinell hardness measurement was made on the matrix of

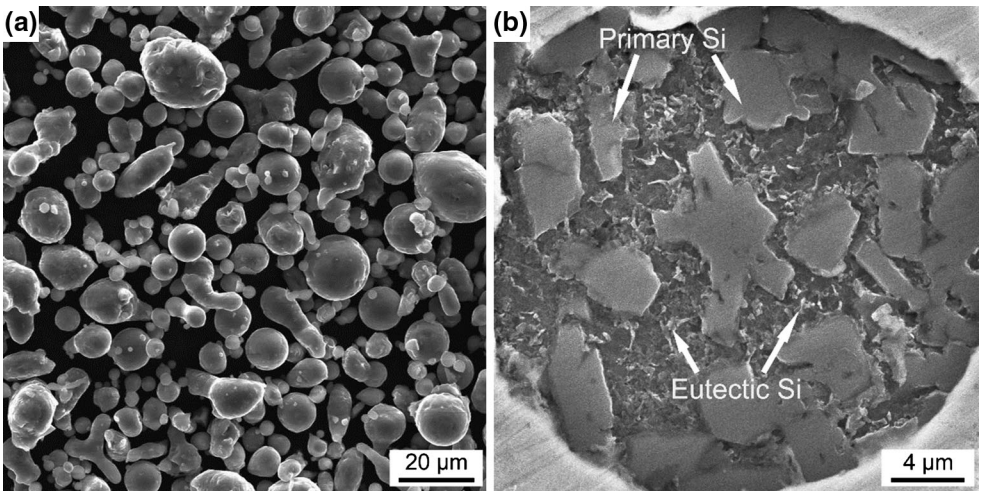

Fig. 1 SEM morphology (**a**) and cross-sectional microstructure (**b**) of the Al–50Si pre-alloy powder prepared by gas atomization

composite away from the reinforcing phase and performed with a load of 7.35 kN and holding time of 30 s. Each datum was the average of three tests or more.

3 Results and discussion

3.1 Microstructural characterization

Figure 2a–c show the hot pressed Al/Sip composites with defect-free microstructure. It can be seen that Si particles distribute homogeneously in Al matrix as a result of using pre-alloyed powder as raw material. No Al–Si eutectic is found. For Al/27Sip composite, most of the Si particles are separated randomly among the matrix. The Si particles are more interconnected with each other as the Si content increases. This phenomenon is different from the conventional metal matrix composites (MMCs) reinforced with ceramic particles, such as Al/SiCp composites [6, 8]. Regardless of the locally connected Si particle, few closed Al regions are observed, even for Al/70Sip composite. Generally, continuous Al matrix is needed for obtaining high thermal and electronic conductivity owing to the good properties of the Al matrix as compares with the Si phase. Meanwhile, the average size of the Si particles increases with the Si content. The size of the Si particles in Al/50Sip composite is in the ranges of 5–18 μm, which is comparable to that manufactured by spray deposition followed by hot isostatic pressing (HIP) [9].

The average density of Al/27Sip, Al/50Sip, and Al/70Sip composite is 2.60, 2.50, and 2.43 g cm^{-3}, respectively. By compare with the theoretical density obtained from the rule of mixture (ROM), full dense composites are achieved. It is worth noting that the densities are only about 82, 30, and 14 % of the Al/70 vol% SiCp composite, Kovar alloy, and Cu/85W composite, respectively. This is desirable in applications which require a light weight. Such result indicates that the current hot pressing process with

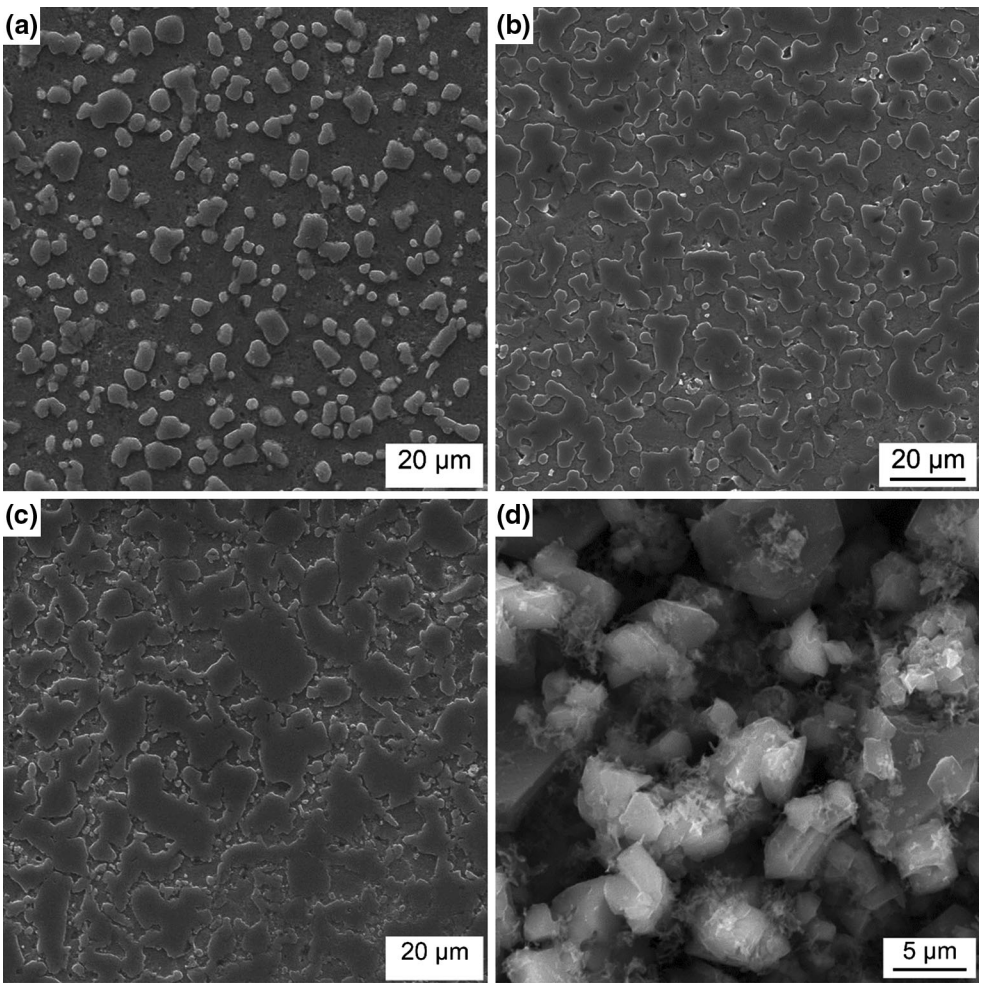

Fig. 2 SEM microstructure of the hot pressed Al/Sip composites: Al/27Sip (**a**), Al/50Sip (**b**), Al/70Sip (**c**), and morphology of the Si particles extracted from the Al/50Sip composite (**d**)

pre-alloyed powder is a feasible method to fabricate Al/Sip composites.

The Al/50Sip composite is also subjected to deep-etching using 50 vol% HCl solute to remove the Al matrix. The morphology of Si reinforcement phase is displayed in Fig. 2d. Silicon particles with three dimensional network structure are observed. The shape of Si particle is quite smooth according to the cross-sectional microstructure. Such microstructure is favorable for achieving MMCs with good performance because crack is predominantly initiated by fracture of sharp reinforcement due to the thermal stress concentration.

Figure 3a shows the XRD pattern of the Al/50Sip composite. All diffraction peaks can be attributed to Al or Si phase and no additional intermetallic or compound can be observed. Therefore, no detrimental reaction is occurred during the fabrication process. Figure 3b is a representative TEM micrograph of the Al/50Sip composite, showing the interface between Si and Al matrix. The interface is clean and free from any interfacial reaction product. This result indicates that no thermal treatment will occur during cyclic heating/cooling, and results in excellent thermal cycle resistance. The fringes are probably the Moore's fringes. Similar XRD patterns and interface characteristics are observed in the Al/27Sip and Al/70Sip composites.

3.2 Thermo-physical properties

Figure 4 shows the CTE values vary with temperature of the Al/Sip composites. It is clear to see that the CTE of the composite decreases significantly as the Si content increases. The good wettability between Al and Si results in good bonding between the Al matrix and the Si reinforcement phase, which effectively hinders the thermal expansion of the matrix. It can be observed that the CTEs increase with the temperature at a decelerating rate. This phenomenon is resulted from the combined role of the solubility of Si in Al and the change of stress on the matrix when the temperature increases [6, 13]. According to the Al–Si phase diagram, the concentration of Si in the Al rises as temperature increases. In the Al matrix, increasing solid solubility of Si has a negative effect on CTE because the lattice parameter of Al decreases with the increase of Si solubility, and the change in lattice parameter and macroscopic length is equal in the case of dilute solid [14]. Thus, the increasing rate of CTE of the Al/Sip composites decreases when the temperature increases beyond a certain point (about 250 °C).

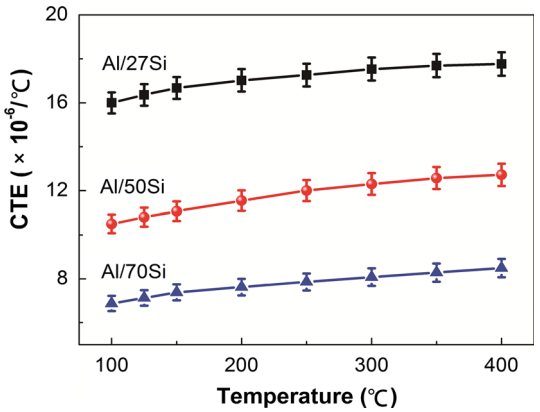

Fig. 4 The variation of CTE as a function of temperature for the hot pressed Al/Sip composites

Another reason for the change of CTE with temperature is the change of stress within the composites. A residual thermal stress will be generated in the composites during cooling from the fabrication temperature due to the large difference in CTE between the Si particle and the Al matrix [9]. Residual stress exhibits as compressive stress on the Si particle and tensile stress on the Al matrix. Thus, during heating from room temperature, the tensile stress on the matrix is relieved and the matrix is expanded, while at the

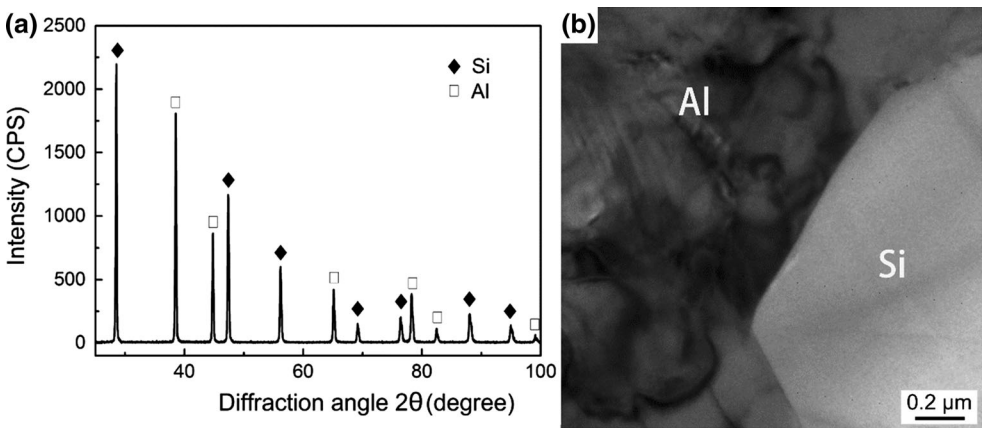

Fig. 3 XRD pattern (**a**) and TEM micrograph of the interface (**b**) of the Al/50Sip composite

same time it helps the expansion of the matrix. When the tensile stress reduces to zero, a new compressive on the matrix is induced due to the CTE mismatch, and this in turn results in decreasing the CTE of the matrix [15]. Although the level of stress on the Si particle is opposite to the Al matrix, its effect on the CTE of the composites can be ignored because of the large modulus and strength of the Si phase. Thus, it is almost impossible for the stress to affect the CTE.

High thermal conductivity is one of the key requirements for electronic packaging material in order to keep low operating temperature and to avoid device failure caused by over-heating. It is generally known that the thermal conductivity of MMCs is influenced by several factors such as volume fraction, geometric distribution, interfacial bonding strength, and thermal conductivity of each component [8]. Thermal conductivity can be calculated by the following formula:

$$\lambda = \alpha \cdot C_p \cdot \rho \quad (1)$$

where λ, α, C_p, and ρ are thermal conductivity, thermal diffusion coefficient, specific heat, and density of the Al/Sip composites, respectively.

Table 1 presents the average thermo-physical properties of the Al/Sip composites and other related materials. The thermal properties decrease with increasing the Si content owing to the lower thermal conductivity of Si phase as compares with Al matrix. The Al/50Sip composite has a thermal conductivity of 146 W m^{-1} K^{-1}, which is higher than that fabricated at 520 °C for 120 min (~130 W m^{-1} K^{-1}) [16] due to the use of high purity Al and Si. This value is near to that of Al/70 vol% SiCp prepared by squeeze casting (~165 W m^{-1} K^{-1}) [8]. In the present work, the high thermal conductivity is also attributed to their high dense and uniform microstructure. The thermal conductivity of MMCs is also influenced by the defects, such as micro-pores. The pores in the composite will decrease the overall thermal conductivity because the air is a poor thermal conductor. The hot pressing of pre-alloyed powder leads to a dense microstructure and guaranteed the thermal conduction capability of the composites. Furthermore, the thermal conductivity/density ratio of the Al/Sip composites (46.9–68.5) is several times larger than the traditional thermal management materials, especially the Cu/85W composite (10.8) [17].

3.3 Mechanical properties

Mechanical properties of the composites are also critical for thermal management applications. Figure 5 shows the tensile curves of four Al/50Sip specimens. It can be seen that the elastic deformation is significant. However, no obvious yield deformation with low elongation is observed, indicating characteristic of brittle fracture. In addition, the curves have a similar stress–strain relation, showing the consistency of the four specimens. The average tensile strength, elastic modulus, and bending strength of the specimens are listed in Table 2. It is seen that the mechanical properties are gradually improved with increasing the Si content. However, obvious plastic deformation is

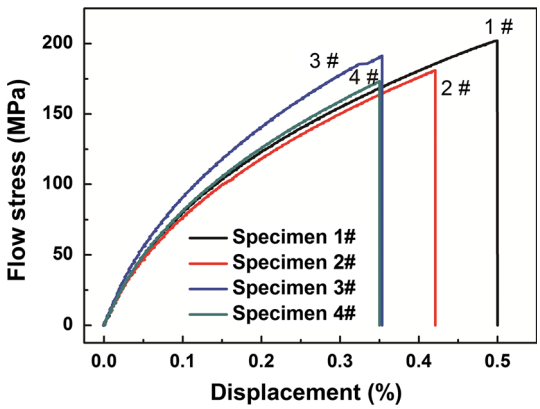

Fig. 5 Tensile flow stress and strain curves of the Al/50Sip composites

Table 1 Thermo-physical properties of the Al/Sip composites and other related materials

Materials	Processing method	Density (g cm^{-1})	Thermal diffusion coefficient (×10^{-6} m^2 s^{-1})	Specific heat (J g^{-1} K^{-1})	Thermal conductivity (W m^{-1} K^{-1})	Note
Al/27Sip	Hot pressing	2.60	77.8	0.88	178	
Al/50Sip	Hot pressing	2.50	68.1	0.85	146	
Al/70Sip	Hot pressing	2.43	57.9	0.81	114	
Al/50Sip	Hot pressing	2.51			130	Ref. [16]
Al/45Si	Liquid–solid separation	2.49	57.4	0.84	120	Ref. [18]
Al/65Sip (vol%)	Infiltration + hot pressing	2.35	66.8	0.79	124	Ref. [19]
Cu/85W	Pressureless sintering	16.7	7.2	0.17	180	Ref. [17]
Al/70SiC (vol%)	Squeeze casting	3.04			165	Ref. [8]

Table 2 Measured mechanical properties of the Al/Sip composites

Properties	Al/27Sip	Al/50Sip	Al/70Sip
Tensile strength (MPa)	149	172	193
Elastic modulus (GPa)	95	105	112
Bending strength (MPa)	213	288	331
Brinell hardness	69	141	167

only observed in the Al/27Sip composite. This result suggests that the mechanical properties of the Al/Sip composites are sufficient to support the semiconductor materials. Moreover, the composites are not unduly hard (Brinell hardness of 69–167), and thus they are amenable to standard machining operations (such as milling and drilling).

3.4 Technological properties

Surface plating is often necessary to increase the wettability between solder and composite; hence improving the welding capacity of the composite. Since Al/Si composite is made up of two different phases, an electroless Ni coating is established using procedures similar to those used for Al alloys. Accordingly, metallized ceramic substrates can be soldered to the composite. The SEM micrograph of Ni coating on Al/50Sip composite is shown in Fig. 6a. It can be seen that the Ni coating is continuous and free of blister. The following isothermal exposure and thermal cycling tests demonstrate that the Ni surface can withstand after 250 °C bake for 30 min or 30 thermal cycles between room temperature and 250 °C. This result shows good adherence between the electroless Ni coating and the composite.

Figure 6b shows the electronic packaging housing made from Al/Sip composites fabricated by rapid solidification and hot pressing method. The housing demonstrates that the composites could be machined successfully by carbide tool into complex components (unlike Al/SiC composite). The right specimen has a wall thickness of 1.0 mm. Additionally, threaded holes with a diameter of 0.5 mm could also be successfully machined on the specimens. Therefore, the Al/Sip composites have received growing interesting in the precision machined components due to their good machinability.

Figure 7a shows the surface appearance of the Al/50Sip composite readily joined by laser welding. It is observed that the keyhole width is about 0.8 mm and the surface appearance of weld is relatively smooth. Figure 7b shows the cross-sectional microstructure of the welding joint which exhibits a fine and homogeneous structure with crack-free. It is reported that the hermetic sealing is also possible using laser welding and diffusion bonding of 4047 or 6061 lids to the Al/Sip composites [20]. Therefore, for the Al/Sip composite, full penetration welds with perfect appearance are obtained by laser welding.

4 Conclusions

Aluminum matrix composites reinforced with different amounts of Si particle were fabricated by rapid solidification and hot pressing method. The microstructure, thermomechanical, workability, platability, and laser weldability were investigated.

1. The rapid solidification followed by hot pressing method was feasible for fabrication of Al/Sip composites with homogeneous and defect-free microstructure. The Si particle was found to be more interconnected with each other as the Si content increased. No interfacial reaction was detected in the composites.

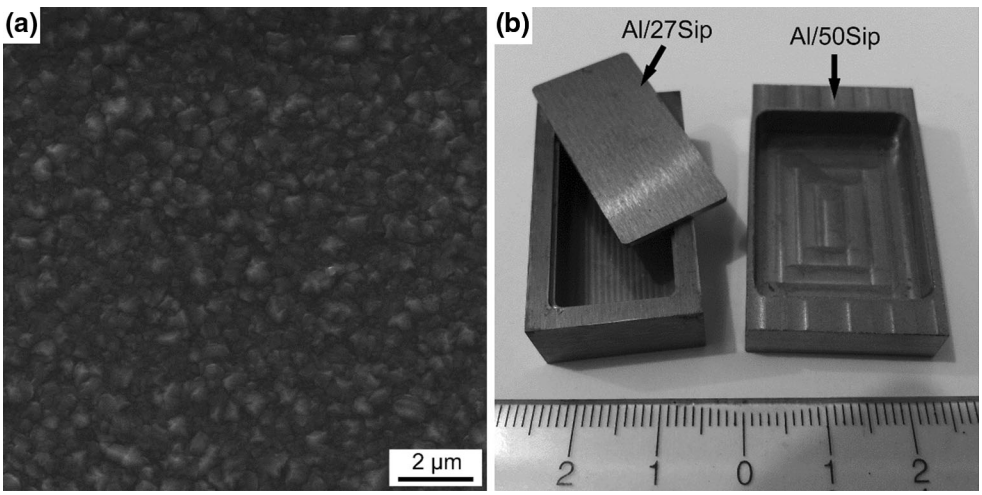

Fig. 6 SEM micrograph of electroless Ni coating (**a**) and electronic packaging housing made by the Al/50Sip composite (**b**)

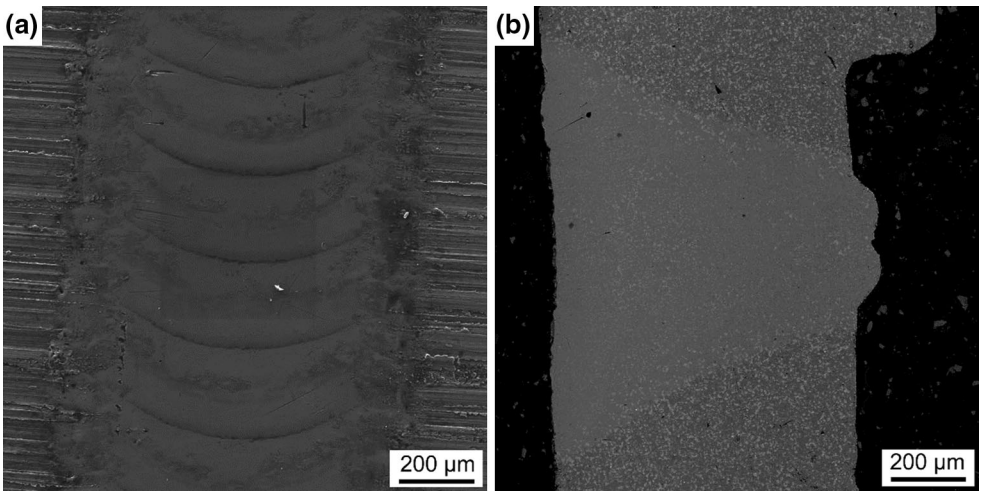

Fig. 7 Surface appearance (**a**) and cross-sectional microstructure (**b**) of the Al/50Sip composite joined by laser welding

2. The measured thermo-physical and mechanical properties of the Al/Sip composites show better performance over the traditional metallic packaging materials, especially the thermal conductivity/density ratio. These properties of such material is suitable for thermal management applications.
3. An electroless Ni coating with densely and uniform microstructure is established on the Al/50Sip composite, which is acceptable for conventional machining. Additionally, the composites can be machined into complex component and can be joined by laser welding.

Acknowledgments The authors would like to thank for the financial support from the National Key Fundamental Research Project of China (JPPT-125-14).

References

1. J.H. Yu, C.B. Wang, Q. Shen, L.M. Zhang, Mater. Des. **41**, 198–202 (2012)
2. C. Zweben, JOM **50**, 47–51 (1998)
3. S.C. Hogg, A. Lambourne, A. Ogilvy, P.S. Grant, Scr. Mater. **55**, 111–114 (2006)
4. M. Schöbel, W. Altendorfer, H.P. Degischer, S. Vaucher, T. Buslaps, M.D. Michiel, M. Hofmann, Compos. Sci. Technol. **71**, 724–733 (2011)
5. X.H. Qu, L. Zhang, M. Wu, S.B. Ren, Prog. Nat. Sci. Mater. Int. **21**, 189–197 (2011)
6. Q. Zhang, G. Wu, L. Jiang, G. Chen, Mater. Chem. Phys. **82**, 780–785 (2003)
7. M. Kida, L. Weber, C. Monachon, A. Mortensen, J. Appl. Phys. **109**, 1–8 (2011)
8. Q. Zhang, L. Jiang, G. Wu, J. Mater. Sci.: Mater. Electron. **25**, 604–608 (2014)
9. Y. Jia, F. Cao, S. Scudino, P. Ma, H. Li, L. Yu, J. Eckert, J. Sun, Mater. Des. **57**, 585–591 (2014)
10. Y.Q. Liu, S.H. Wei, J.Z. Fan, Z.L. Ma, T. Zuo, J. Mater. Sci. Technol. **30**, 417–422 (2014)
11. T.S. Srivatsan, T.S. Sudarshan, E.J. Lavernia, Prog. Mater. Sci. **39**, 317–409 (1995)
12. P.J. Ward, H.V. Atkinson, P.R.G. Anderson, L.G. Elias, B. Garcia, L. Kahlen, J.M. Rodriguez-ibabe, Acta Mater. **44**, 1717–1727 (1996)
13. T.A. Hahn, R.W. Armstrong, Int. J. Thermophys. **9**, 179–193 (1988)
14. S. Ren, X. He, X. Qu, I.S. Humail, Y. Li, Mater. Sci. Eng. B **138**, 263–270 (2007)
15. C.R. Berry, J. Appl. Phys. **24**, 658–659 (1953)
16. G. Mi, C. Li, K. Wang, L. Chen, Mater. Res. Innovations **17**, 182–185 (2013)
17. S.H. Lee, S.Y. Kwon, H.J. Ham, Thermochim. Acta **542**, 2–5 (2012)
18. Y. Li, J. Liu, W. Wang, G. Liu, Trans. Nonferrous Met. Soc. China **23**, 970–976 (2013)
19. X. Wang, G. Wu, R. Wang, Z. Xiu, K. Yu, Trans. Nonferrous Met. Soc. China **17**, 1039–1042 (2007)
20. Sandvik Osprey Ltd, (2014). http://www.cealloys.com/tech_info.htm